International Conference on Green Energy & Environmental Engineering (GEEE-2018)
Proceedings of Engineering and Technology – PET
Vol.37 pp.50-57

Control and Filter Design of Single Phase Grid-Connected Inverter for PV applications

Meriem Dardouri[#1], Sejir Khojet el Khil[#1], Khaled Jelassi[#1]

[#1] *Université de Tunis EL Manar, LSE-ENIT, ENIT-L.S.E, LR 11 ES 15, BP 37, 1002 Tunis, Tunisia*
meriem.dardouri@enit.utm.tn
sejirkek@gmail.com
khaled.jelassi@enit.utm.tn

***Abstract*— Solar power represents an important potential that has been widely exploited over the last years. For PV-Grid connected applications, the grid current has to be controlled in a way that ensure sinusoidal current injection to meet all standards regarding grid-tied systems. This paper presents the control strategy of a single-phase LCL-Filter grid connected inverter for PV applications. Firstly, PV system and P&O MPPT technique are presented followed by a three grid interfacing passive filters topologies comparison in order to validate the performance and effectiveness of each one. It is then shown that the LCL-Filter provides better harmonic attenuation also a filter size reduction. In addition, this paper suggests a design procedure as well as a passive damping method to avoid instability problems caused by LCL-Filter resonance peak. Furthermore, a control strategy based on a PI-PR controllers combination is introduced to provide high power quality. Several simulations tests are presented to validate the effectiveness of the proposed control procedure for a 4kW PV grid-connected inverter.**

***Keywords*— PV panel, MPPT, L-LC-LCL Filters, harmonic distortion, passive damping, PI-PR controllers, grid-connected inverter.**

NOMENCLATURE

V_g	Grid voltage
V_{dc}	DC-link voltage
V_{inv}	Inverter voltage
V_c	LCL-Filter capacitor voltage
f_g	Grid frequency
i_g	Grid current
i_c	LCL-Filter capacitor current
i_1	Inverter current
L_{ci}	Inverter side inductance
L_{cg}	Grid side inductance
C_f	LCL-Filter capacitor
R_d	Damping resistor
C_{dc}	DC-link capacitor
Z_g	Grid impedance
I_{pv}	PV cell current
V_{pv}	PV cell output voltage
I_{ph}	Current generated by the incident light
I_0	Diode reverse saturation current
V_t	PV Cell thermal voltage
R_s	PV cell serial resistance
R_p	PV cell parallel resistance
N_s	Number of PV panel series cell
N_p	Number of PV panel parallel cell
a	diode ideality constant

I. INTRODUCTION

For too long fossil fuels have met most of the world's energy need. However, they are environmentally damaging techniques and of high cost. Therefore, renewable energy such as wind, sun, biomass,… have arisen as attractive solution since they are environmental friendly and inexhaustible sources of energy. Out of these, PV energy is perhaps the right direction considering that in an hour, the sun radiates solar clean energy enough to cover human energy consumption for a year, which makes it one of these resources that has undergone very quickly growth lately[1]-[2]. However, some factors like solar radiance temperature as well as the non-linearity of the PV cells affect the PV system performance [3].

To reduce these challenges effects, a maximum power tracking MPPT algorithm is generally used as an effective technique for maximum power extraction [4].

The connection of the PV source to the main grid requires the use of power electronics converters since they gives good results and performances [5]. Depending on the nature of the source, several conversion chains are used. In all cases, the output stage is similar and consists of a controlled voltage inverter injecting sinusoidal current to the grid. However, the switching of the power conversion devices causes high frequency harmonics, which is why the used converter is usually connected to the grid via passive filters. Even though its simple structure and control strategy, L filter is considered voluminous and inefficient in order to satisfy harmonic standard regulations stated in IEEE-1547 [6]. To overcome this issue, high order filters were introduced as a solution and more precisely LCL filters thanks to its low cost as well as its excellent harmonic suppression ability [7]. However, it provides an unwanted resonance effect that generates stability problems. In order to solve this, many techniques have been proposed to damp this unwanted resonance, including passive [8] and active damping [9]. Furthermore, high performances operating in terms of injected grid current is essential for DC/AC converters.

This paper proposes a simple and effective control strategy for single-phase grid-tied LCL filter VSI. The proposed structure, shown in Fig.1, is composed of two cascaded regulation loops resulting in a robust and well-damped control system. The paper also deals with the design procedure of the passive damped LCL filter as well as a comparison of ideal-PR

ISSN 2356-5608

International Conference on Green Energy & Environmental Engineering (GEEE-2018)
Proceedings of Engineering and Technology – PET
Vol.37 pp.50-57

and non-ideal-PR controllers is presented based on both performances.

II. System Overview

The proposed work presents agrid connected PV system for residential application. Fig.1 shows the typical structure of a two-stage single-phase grid-connected photovoltaic (PV) system.

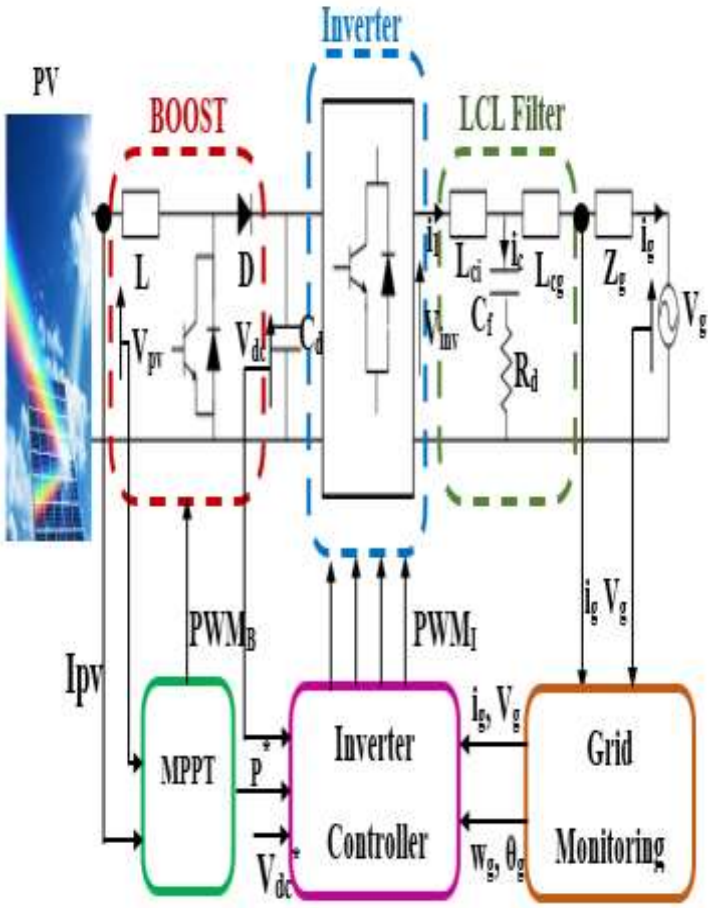

Fig. 1. Control structure of the single-phase grid connected photovoltaic (PV) system

The LCL filter composed of series connected L_{ci}, L_{cg} and C_f + R_d is used to attenuate the harmonic injected into the grid caused by the switching of the inverter switches. The VSI's function is to inject a sinusoidal current in the grid with unity power factor.

According to Fig.1, the VSI mathematical model is as follow:

$$\begin{cases} L_{ci}\frac{di_1}{dt} = V_{inv} - V_c - R_d i_c \\ L_{cg}\frac{di_g}{dt} = V_c - V_g - R_d i_c \\ C_f\frac{dv_c}{dt} = i_c \\ i_1 = i_g + i_c \end{cases} \quad (1)$$

The PV system draws the maximum power from the PV panel (MPPT operation) and transfers it to the grid with high quality power using different control techniques. The most used control strategies in single-phase inverters has two cascaded control loops. The inner loop is a current loop, the outer loop is a voltage control loop, in which the voltage of the DC-side can be ensured, and a reference of the inner current loop is calculated simultaneously in the outer loop.

III. PV System Control

The PV panel is a set of series (N_s)-parallel (N_p) connected pv cells. Thus, modelling a PV panel is modelling a simple pv cell. This section analyzes at first the electrical part of a PV panel through the study of the equivalent circuit of the ideal PV cell and the fundamental equations that describe it and presents next the P&O MPPT technique

A. Photovoltaic cell model

The pv cell, as reported in Fig.2, consists of a current source in parallel with a diode D and series and parallel resistances R_p, R_s

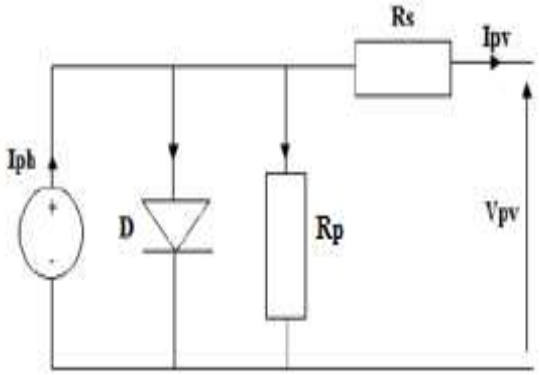

Fig.2. Equivalent circuit of solar pv cell

The basic equation describing the I_{pv}–V_{pv} characteristic of the ideal PV is expressed by the following expression [10]:

$$I_{pv} = I_{ph} - I_0[\exp\left(\frac{V_{pv}+R_s I_{pv}}{V_t a}\right) - 1] - \frac{V_{pv}+R_s I_{pv}}{R_{sh}} \quad (2)$$

For a PV panel series cells and N_p parallel cells, the expression (2) turns into [14]:

$$I_{pv} = N_p I_{ph} - N_p I_0[\exp\left(\frac{\frac{V_{pv}}{N_s}+\frac{R_s}{N_p}I_{pv}}{V_t a}\right) - 1] - \frac{\frac{N_p}{N_s}V_{pv}+R_s I_{pv}}{R_{sh}} \quad (3)$$

B. Maximum Power Point Tracking

The amount of maximum power that can be extracted from the PV panel at a given time is a function of the solar irradiance and the ambient temperature which are continuously changing so a maximum power tracking algorithm is necessary. Perturb and observe (P&O) algorithm is simple and the most widely used MPPT algorithm, illustrated by Fig.3, because of its balance between performance and simplicity [11].

The P&O algorithm is based on the application of a perturbation to the system and detecting the PV panel output power variation. The duty cycle of the DC-DC converter is then varied and the process is repeated until the maximum power point is reached.

ISSN 2356-5608

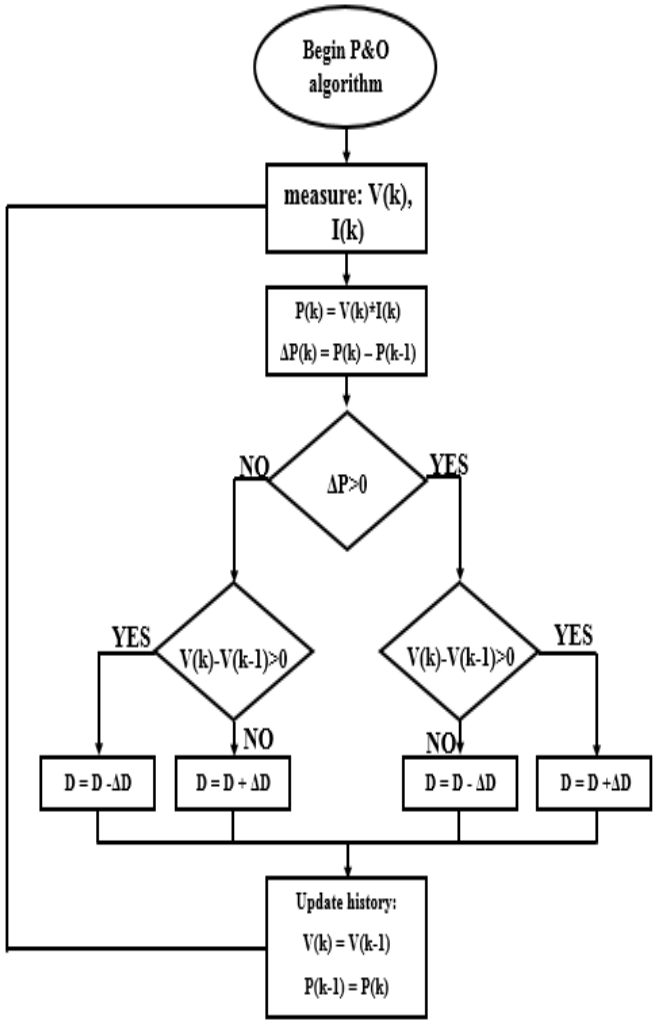

Fig.3 P&O algorithm flowchart

IV. GRID INTERFACING

A. *Filters topologies*

This part discusses different types of grid connection's filter. In the literature, three filters were proposed:

- First order L Filter;
- Second order LC Filter;
- Third order LCL Filter;

In order to choose the optimal filter topology, filters with reduced power losses and high attenuation performance have priority.

- L Filter: a first order filter that has a -20db/decade attenuation. The transfer function of the L filter is:

$$H_L(s) = \frac{1}{Ls+R} \quad (4)$$

- LC Filter: a second order filter that has a -40db/decade attenuation and presents a peak at the resonance frequency F_{res}. The transfer function of the LC filter is:

$$H_{LC} = \frac{1}{LCs^2+1} \quad (5)$$

- LCL Filter: a third order filter that has a -60db/decade attenuation and also presents a resonance peak. The transfer function of the LCL filter is:

$$H_{LCL} = \frac{1}{L_{ci}L_{cg}C_f s^3+(L_{ci}+L_{cg})s} \quad (6)$$

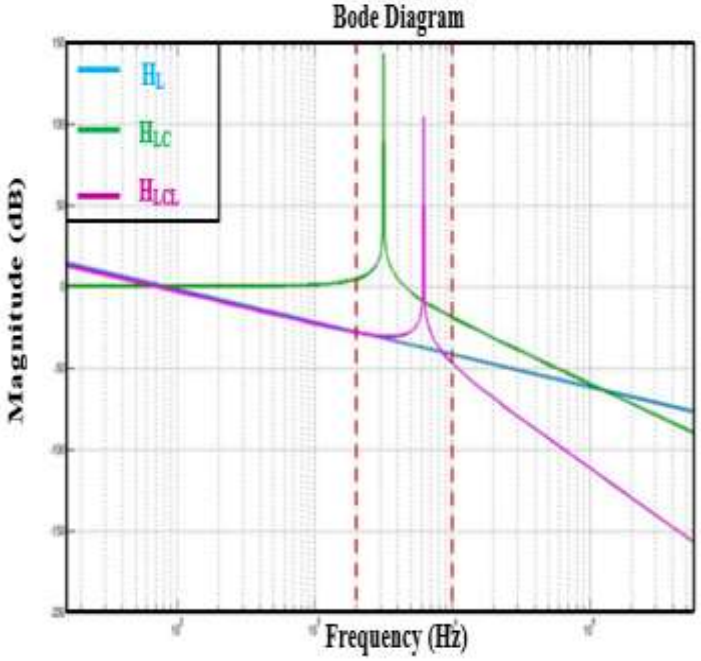

Fig. 4. Harmonic Attenuation of L, LC, LCL Filters

In Fig.4 is reported the Bode diagram of the three filters: At low frequencies, LCL and L filters present a similar attenuation behavior. LC and LCL filters present both a large resonance peak in the second zone, which can cause instability to the system while L filter offers better attenuation. For high frequencies, LCL filter has a better attenuation than that L and LC filter and it is in this zone where lies its interest.

When taking into consideration cost, weight and harmonic attenuation, LCL filter seems to be more suited for our application but it presents resonance peak which can be eliminated by a passive damping strategy.

B. *LCL filter design procedure*

Due its resonance peak, LCL filter must be designed precisely according to the parameters of the inverter. The design procedure of the LCL filter is inspired from [12].

The first step in the process of designing LCL filter parameters is the calculation of the basic impedance Z_b and filter capacity C_b values as indicated below [12]:

$$Z_b = \frac{V_g^2}{P_n} \quad (7)$$

$$C_b = \frac{1}{w_g Z_b} = \frac{1}{2\pi f_g Z_b} \quad (8)$$

The main LCL-Filter design steps are summarized in Fig.5

ISSN 2356-5608

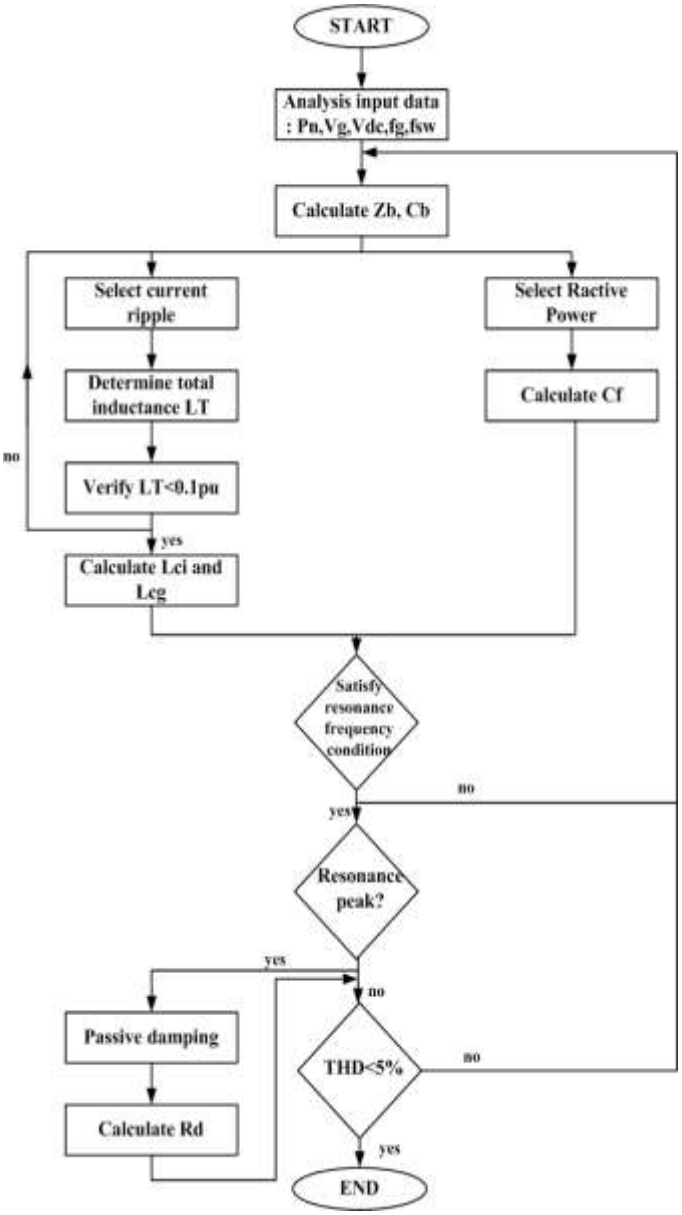

Fig. 5. LCL-Filter design procedure

1) Filter Capacitor Calculation:

Standards require a quasi-unit power factor. Thus, the reactive power consumed by the filter capacity must be less than λ% (the reactive power factor generally less or equal to 5) of the active power of the system in order to avoid a decrease in the power factor [20].

The filter capacitor C_f can then be determined as following [13]:

$$C_f = \frac{Q_c}{V_g^2 w_g} = \frac{\lambda P_n}{V_g^2 w_g} \quad (9)$$

2) Filter Inductance Calculation:

The reduction of the current harmonics is done in accordance with the IEEE 519-1992 standard [14]. The value of the total inductance L_{Tmax} given by equation (10) must be less than 10% of the value of the basic inductance L_{Tb}. In fact, small values of L_{ci} and L_{cg} make it possible to reduce the voltage drop of the LCL filter while large values allow to obtain a filter that is not only bulky but also more expensive.

$$L_{Tmax} = (L_{ci} + L_{cg})_{max} = 10\%\, L_{Tb} = 10\% \frac{Z_b}{2\pi f_g} \quad (10)$$

The inverter side inductance is given by the following expression: [15]

$$L_{ci} = \frac{V_{DC}}{6\, f_{sw} \Delta I_{L-max}} \quad (11)$$

Where Δ*IL* max is the 10% current ripple specified by [16]:

$$\Delta I_{L-max} = 0.1\, \frac{\sqrt{2} P_n}{V_g} \quad (12)$$

The grid side inductance can be then deduced from the equation (10) Finally, after designing the filter, the resonant frequency must be calculated to ensure that it satisfies the third limitation of the LCL filter sizing procedure.

C. LCL-Filter Passive Damping

Passive damping methods gain a lot of interest because of their simplicity, cost and simple implementation. Simple series passive damping is considered as the simplest and most adopted method for LCL filter resonance damping [17]. It is obtained by introducing a series resistor with the filter capacity C_f (Fig.6).

The transfer function of the series R_d damped LCL filter is expressed by the following equation:

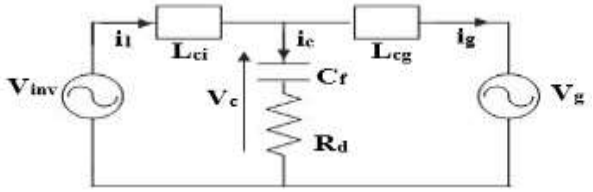

Fig. 6. Simple series resistor Passive Damping

$$H_{Rd} = \frac{1 + R_d C_f s}{L_{ci} L_{cg} C_f s^3 + (L_{ci} + L_{cg}) R_d C_f s^2 + (L_{ci} + L_{cg}) s} \quad (13)$$

The stability of the system is analyzed based on the Bode diagram of the transfer function H_{Rd} reported in Fig.7

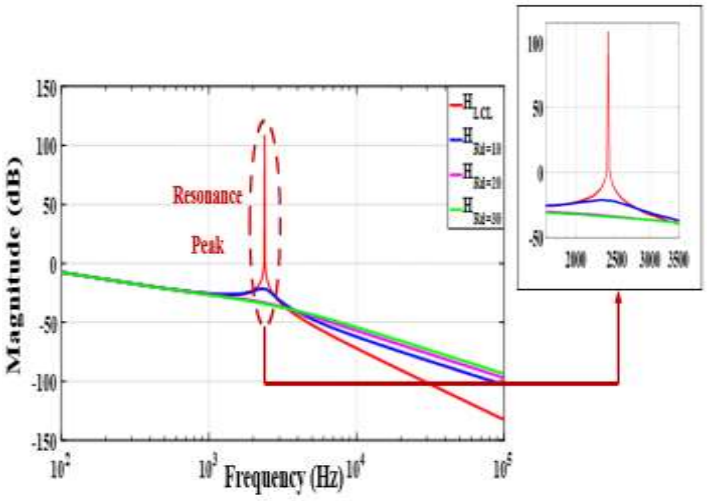

Fig. 7. Bode Diagram Plot of LCL Filter for different values of R_d

ISSN 2356-5608

Fig.5 shows the Bode diagram of the LCL filter transfer function for different values of the damping resistor. As shown in this figure, the higher is the damping resistor, the more the filter resonance is attenuated. The appropriate value of the damping resistor R_d can be calculated by setting the resonance pulsation and the filter capacity as follows: [18]

$$R_d = \frac{1}{3w_{rés} * C_f}$$

V. CONTROL STRATEGY

The aim of control of the grid connected inverter is to ensure a sinusoidal current injection in the grid, a constant dc-link voltage as well as a unity power factor.

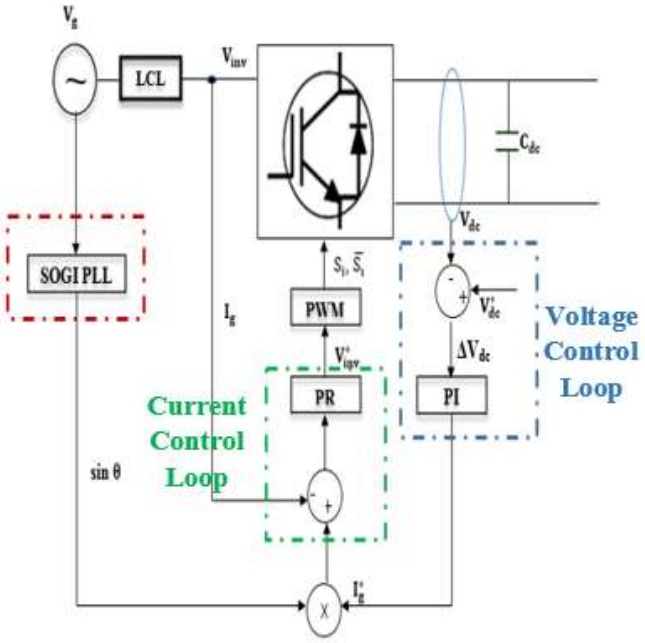

Fig. 8. The inverter control strategy

Fig.8 explains the control strategy: it includes an external PI control loop for the output current regulation, stabilized by an inner PR control loop for the inverter current: the output voltage error ΔV_{dc} is fed to a PI regulator, which generates reference current I_g^*. The PWM inverter is then modulated according to the out of the PR controller.

A. *Grid Monitoring*

Different methods using different techniques for monitoring the grid voltage are presented in the literature. Among these, the second-order generalized integrator-based PLL (SOGI-PLL) is an effective approach thanks to its fast dynamic response, high filtering capacity,…[20].

B. *Voltage Control Loop*

The main purpose of the dc-link voltage control loop is to maintain this voltage at a constant reference value while ensuring a zero state error. The voltage control loop is based on a simple PI controller since it is simple, easy to implement and present good results when regulating DC-quantities.

C. *Current control Loop*

Current controller performance determines the performance of the overall system. In the literature, many control methods have been proposed especially PI and PR controllers. PI controllers are used in order to control the DC-quantities while PR controllers are used to control the AC-quantities [19].

In fact, PI current controller has a considerable steady state error when following the reference current while the steady state error is less for the PR current controller, practically negligible. The PR current controller $C_{PR}(s)$ is represented by [19]:

$$C_{PR\_ideal}(s) = K_p + \frac{K_i s}{s^2 + w_0^2} \quad (15)$$

The main drawback is the ideal PR controller infinite gain that can cause instability. This shortcoming can be avoided by using a non-ideal PR controller as showing in the following expression [19]:

$$C_{PR\_nn\_ideal}(s) = K_p + \frac{K_i w_c s}{s^2 + 2w_c s + w_0^2} \quad (16)$$

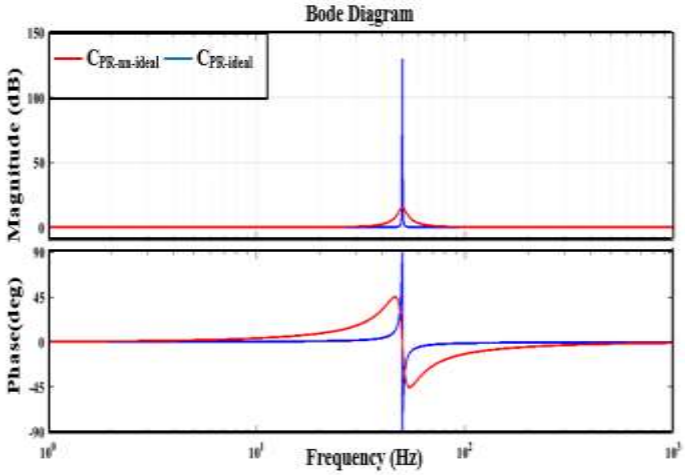

Fig. 9. Bode plots of ideal and non-ideal PR controllers

In Fig.9 is reported bode plot of both ideal and non-ideal PR controllers: As shown, the ideal PR controller presents an infinite gain while the gain of the non-ideal PR controller at the AC frequency ω_0 is finite but it is still large enough to provide only a very small steady state error.

The control model of the current corrector can be derived by simplifying the LCL filter into an L filter. [21]

This simplification is justifiable since at low frequencies, the LCL and L filters present a similar behavior (Fig.4-zone1) as well as the impedance of C_f at low frequencies is high so :

- $L_T = L_{ci} + L_{cg} + L_g$ (16)
- $R_T = R_{ci} + R_{cg}$ (17)

To tune the resonant corrector, we used the criterion of the generalized stability margin [22]: to have the best performance of the system several values of the stability margin r have been tested.

VI. SIMULATIONS RESULTS AND DISCUSSION

The overall control startegy of the PV grid-tied inverter with LCL filter passive damping method is studied and analysed using the software Matlab-Simulink in this paper. The system parameters used in this study are illustarted in Table I and the PV panel are presented in Table II

ISSN 2356-5608

TABLE I
SYSTEM PARAMETERS

Grid Voltage V_g [V]	230
Rated Power P_n [w]	4000
Grid Frequency f_g [Hz]	50
Switching Frequency f_{sw} [Hz]	10000
DC Link Voltage V_{DC} [V]	400
Grid side inductance L_{cg} [mH]	1
inverter side inductance L_{ci} [mH]	2
Filter capacitor [μF]	6
Damping resistor R_d [Ω]	3.5

Table II
PV Datasheet

P_{max} [w]	200
I_{mp} [A]	5.43
V_{mp} [V]	36.8
I_{sc} [A]	5.67
V_{oc} [V]	46.43

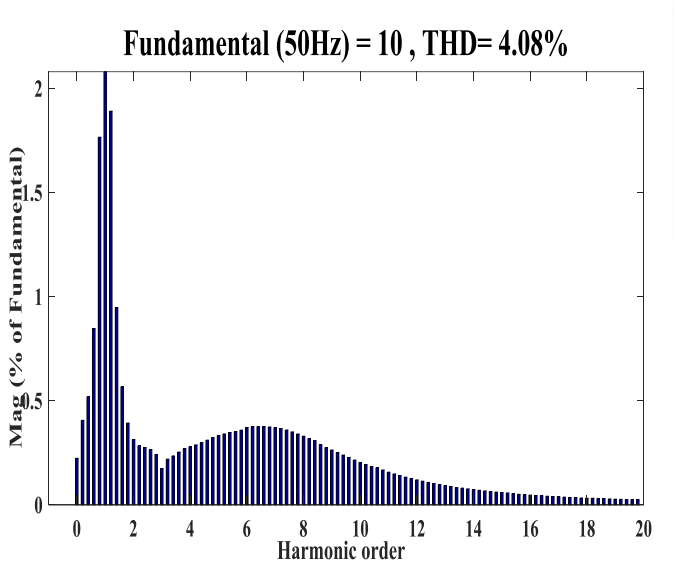

(a)

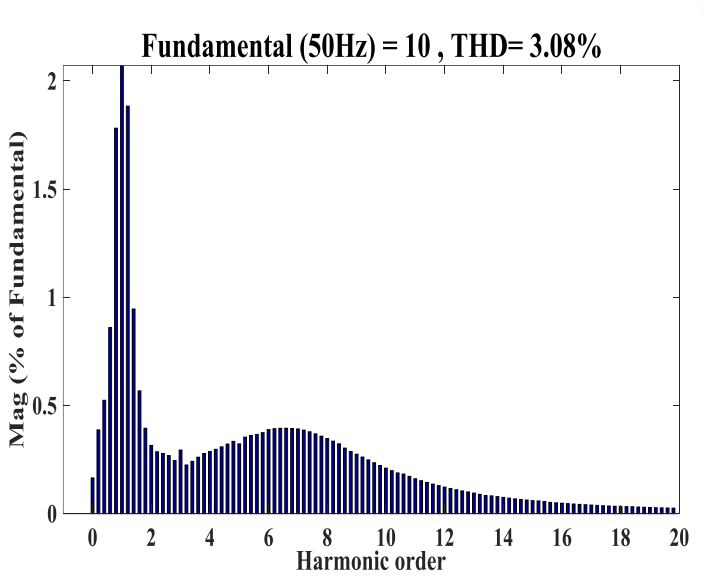

(b)

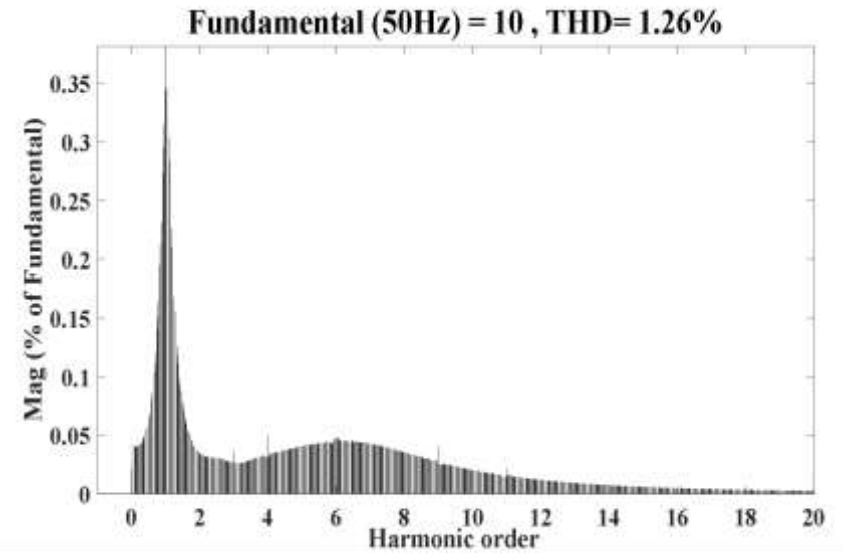

(c)

Fig. 10. Grid current Harmonic spectrum (a) L-Filter (b) LC-Filter (c) LCL-Filter

ISSN 2356-5608

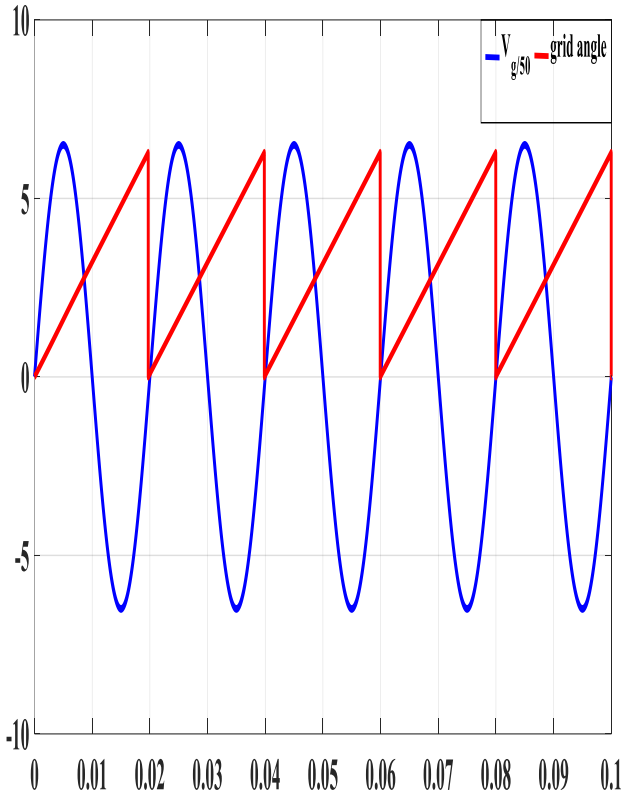

Fig.11. SOGI-PLL simulation results: grid voltage V_g and grid estimated angle θ_g

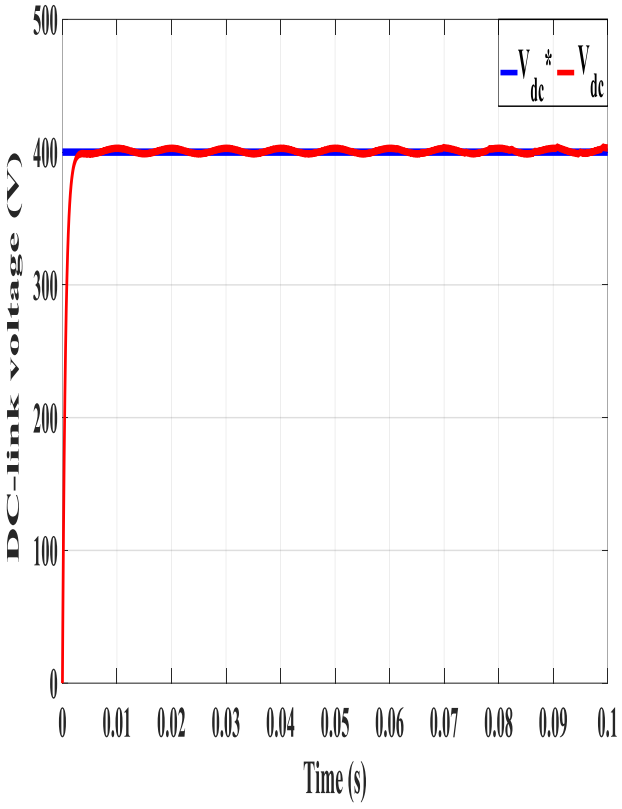

Fig. 13. DC-link voltage control simulation results

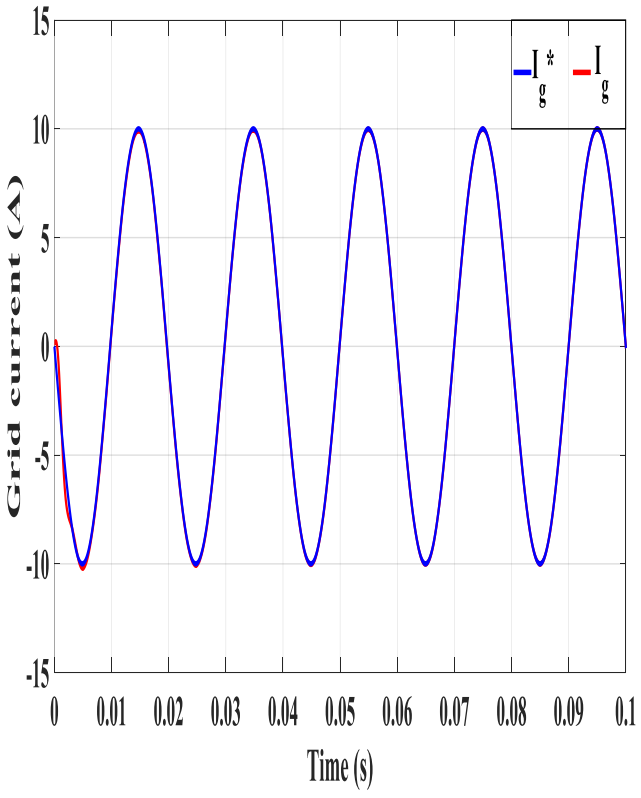

Fig. 12. Grid current control loop simulation results

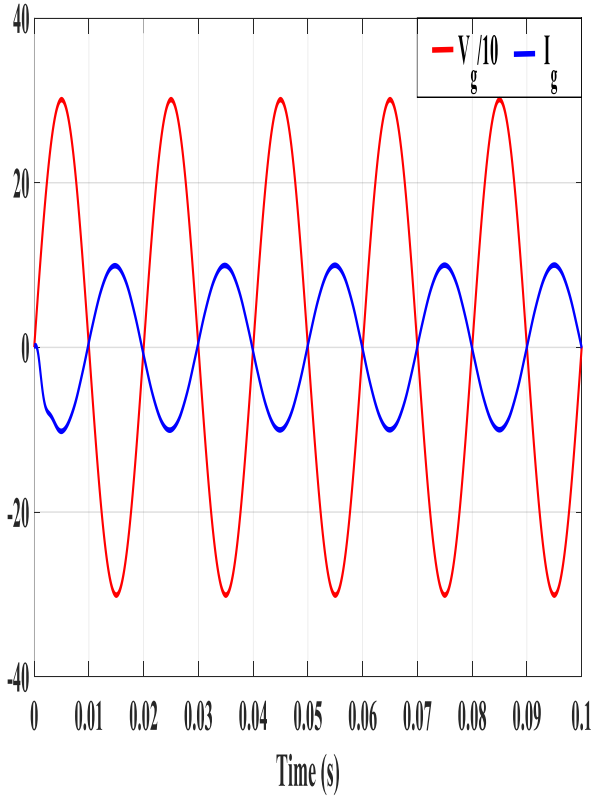

Fig. 14. Grid voltage and current simulation results

ISSN 2356-5608

As shown in Fig.10, the grid current THD improves slightly depending on the adopted grid connection filter. In fact, when using an L-Filter, the THD is of 4.08% (Fig10.a) reduced to 3.08% (Fig10.b) with an LC-Filter and reach finally a value of 1.26% (Fig10.c) with an LCL-Filter. The obtained results confirm then the effectiveness of the LCL-Filter compared to other passive filters topologies.

Fig.11 shows the phase angle obtained with the SOGI-PLL technique : it clearly coincides well with the grid voltage V_g.

From the simulation results shown in Fig.12, using PR controller, the grid current follows its reference presenting a slight steady state error, practically negligible. This insignificant error is a result of the use of the non-ideal PR controller as it provides small steady state error while avoiding the ideal PR controller instability. We therefore see the particular interest of the use of the resonant corrector for the regulation of sinusoidal quantities.

Similarly, from the simulation results shown in Fig.13, the DC-link voltage V_{dc} follows perfectly the reference voltage V_{dc}^*.

In addition, the single-phase waveforms of grid current and grid voltage are presented in Fig.14: The power factor is 0.9999 and since the THD of the grid current is equal to 1.26%, the quality of the grid current is fairly good.

VII. CONCLUSION

This paper proposes a complete control strategy for a single-phase inverter for PV applications with associated controllers operating in LCL-grid-connected mode to ensure high power quality injection along with a low grid current THD and stable dc-link voltage.

The effectiveness of the designed LCL-Filter when attenuating the grid current harmonic distortion has been proven with simulation results.

The control topology based on three control loops: a phase locked loop, an inner PR current control loop and external PI voltage control loop has been presented.

This simple proposed control system has been testes and validated with simulation, which has shown that the system meets requirements and standards.

REFERENCES

[1] M. A. Ghasemi, A. Ramyar and H. Iman-Eini, "MPPT Method for PV Systems Under Partially Shaded Conditions by Approximating I–V Curve," in *IEEE Transactions on Industrial Electronics*, vol. 65, no. 5, pp. 3966-3975, May 2018.

[2] A. Urtasun and D. D. C. Lu, "Control of a Single-Switch Two- Input Buck Converter for MPPT of Two PV Strings," *IEEE Transactions on Industrial Electronics*, vol. 62, pp. 7051-7060, 2015.

[3] A. Costabeber, M. Carraro, and M. Zigliotto, "Convergence Analysis and Tuning of a Sliding-Mode Ripple-Correlation MPPT," *IEEE Transactions on Energy Conversion*, vol. 30, pp. 696-706, 2015.

[4] Seyedmahmoudian, M.; Horan, B.; Soon, T. Kok; Rahmani, R.; Than Oo, A. Muang; Mekhilef, S.; Stojcevski, A. (2016-10-01). "State of the art artificial intelligence-based MPPT techniques for mitigating partial shading effects on PV systems – A review". Renewable and Sustainable Energy Reviews. 64: 435 455

[5] B. K. Bose, "Power Electronics in Smart Grid and Renewable Energy Systems ", in *Proceedings of the IEEE*, vol. 105, no. 11, pp. 2007-2010, Nov. 2017

[6] IEEE Standard for Interconnecting Distributed Resources with Electric Power Systems," in *IEEE Std 1547-2003*, vol., no., pp.1-28, July 28 2003

[7] H. Cha and T. K. Vu, "Comparative analysis of low-pass output filter for single-phase grid-connected Photovoltaic inverter," *2010 Twenty-Fifth Annual IEEE Applied Power Electronics Conference and Exposition (APEC)*, Palm Springs, CA, 2010, pp. 1659-1665.

[8] M. Büyük, A. Tan, K. Ç. Bayindir and M. Tümay, "Analysis and comparison of passive damping methods for shunt active power filter with output LCL filter," *2015 Intl Aegean Conference on Electrical Machines & Power Electronics (ACEMP), 2015 Intl Conference on Optimization of Electrical & Electronic Equipment (OPTIM) & 2015 Intl Symposium on Advanced Electromechanical Motion Systems (ELECTROMOTION)*, Side, 2015, pp. 434-440.

[9] A. Ghoshal and V. John, "Active damping of LCL filter at low switching to resonance frequency ratio," in IET Power Electronics, vol. 8, no. 4, pp. 574-582, 4 2015.

[10] D. Bonkoungou, Z. Koalaga and D.Njomo. "Modelling and Simulation of photovoltaic module considering single-diode equivalent circuit model in MATLAB", Int. Journal of Emerging Technology and Advanced Engineering, pp 493-502, Vol:3, March 2013.

[11] M. A. Elgendy, B. Zahawi, and D. J. Atkinson, "Assessment of perturb and observe MPPT algorithm implementation techniques for PV pumping applications," IEEE Transactions on Sustainable Energy, vol. 3, no. 1, pp. 21–33, 2012.

[12] Liserre, M., Blaabjerg, F., Hansen, S. 2005. « Design and Control of an LCLfilter based Three-phase Active Rectifier ». *IEEE Transactions on Industry Applications*, vol. 41 no 5, p. 1281-1291.

[13] IEEE Guide for Application and Specification of Harmonic Filters," in IEEE Std 1531-2003, vol., no., pp.0_1-60, 2003

[14] 519-1992 IEEE Recommended Practices and Requirements for Harmonic Control in Electrical Power Systems," IEEE Std 519-1992, 1993

[15] A. Reznik, M. G. Simoes, A. Al-Durra, S. M. Muyeen, " LCL filter design and performance analysis for grid-interconnected systems ", *IEEE Trans. Ind. Appl.*, vol. 50, no. 2, pp. 1225-1232, Mar./Apr. 2014.

[16] V. H. Prasad, "Average current mode control of a voltage source inverter connected to the grid: Application to different filter cells," Master's Thesis, Dept. Electrical Engineering., Virginia Tech, Blacksburg, Virginia, 1997.

[17] X .Renzhong, X. Lie, Z .J unjun, and D. Jie "Design and Research on the LCL Filter in Three-Phase PY Grid-Connected Inverters" International Journal of Computer and Electrical Engineering, Yol. 5, No. 3, June 2013.

[18] J. Bauer, " Single Phase Yoltage Source Inverter Photovoltaic Application " Acta Polytechnica Yol. 50 No. 4/2010.

[19] A. Ben Youssef, S. Khojet El Khil, I. Slama-Belkhodja, "State Observer-Based Sensor Fault Detection and Isolation, and Fault Tolerant Control of a Single-Phase PWM Rectifier for Electric Railway Traction", IEEE Trans. Power Electron, vol. 28, no. 12, pp. 5842-5853 2013.

[20] Han, Y.; Luo, M.; Zhao, X.; Guerrero, J.M.; Xu, L. Comparative Performance Evaluation of Orthogonal-Signal-Generators-Based Single-Phase PLL Algorithms—A Survey. IEEE Trans. Power Electron.2016, 31, 3932–3944.

[21] D. N. Zmood and D. G. Holmes, "Stationary frame current regulation of PWM inverters with zero steady-state error," in *IEEE Transactions on Power Electronics*, vol. 18, no. 3, pp. 814-822, May 2003.

[22] J. ZENG, « Contrôle haute performance de machines synchrones à aimants permanents par correcteurs résonnants multi fréquentiels », thèse de Doctorat, Université des Sciences et 38 Techniques de Lille, novembre 2005

ISSN 2356-5608